ORIGINAL ARTICLE

Volume-based and Surface-Based Methods in Autism Compared with Healthy Controls Are Free surfer and CAT12 in Agreement?

How to Cite This Article: Faraji R , Ganji Z, Khandan Khadem Za, Akbari Lalimia H, Eidy F, Zare H. Volume-based and Surface-Based Methods in Autism Compared with Healthy Controls; Are Free surfer and CAT12 in Agreement? Iran J Child Neurol. Winter 2024; 18 (1) :93-118

Reyhane FARAJI PhD [1],
Zohreh GANJI PhD [1],
Zahra KHANDAN KHADEM MD [1],
Hossein AKBARI-LALIMI PhD [1],
Fereshteh EIDY PhD [2],
Hoda ZARE MD [1,3]

1.Medical Physics Research Center, Mashhad University of Medical Sciences, Mashhad, Iran
2.Department of Biostatistics, Faculty of Medical Sciences, Tarbiat Modares University, Tehran, Iran
3.Department of Medical Physics, Faculty of Medicine, Mashhad University of Medical Sciences, Mashhad, Iran.

Corresponding Author
Zare H. MD
Email: zareh@mums.ac.ir
Department of Medical Physics, Faculty of Medicine, Mashhad University of Medical Sciences, Mashhad, Iran

Abstract

Objectives: Autism Spectrum Disorder (ASD) encompasses a range of neurodevelopmental disorders, and early detection is crucial. This study aims to identify the Regions of Interest (ROIs) with significant differences between healthy controls and individuals with autism, as well as evaluate the agreement between FreeSurfer 6 (FS6) and Computational Anatomy Toolbox (CAT12) methods.

Materials & Methods

ISurface-based and volume-based features were extracted from FS software and CAT12 toolbox for Statistical Parametric Mapping (SPM) software to estimate ROI-wise biomarkers. These biomarkers were compared between 18 males Typically Developing Controls (TDCs) and 40 male subjects with ASD to assess group differences for each method. Finally, agreement and regression analyses were performed between the two methods for TDCs and ASD groups.

Results

Both methods revealed ROIs with significant differences for each parameter. The Analysis of Covariance (ANCOVA) showed that both TDCs and ASD groups indicated a significant relationship between the two methods ($p<0.001$). The R2 values for TDCs and ASD groups were 0.692 and 0.680, respectively, demonstrating a moderate correlation between CAT12 and FS6. Bland-Altman graphs showed a moderate level of agreement between the two methods.

Received: 20-Sep-2023
Accepted: 07-Dec-2023
Published: 18-Jan-2024

Conclusion

The moderate correlation and agreement between CAT12 and FS6 suggest that while some consistency is observed in the results, CAT12 is not a superior substitute for FS6 software. Further research is needed to identify a potential replacement for this method.

Keywords: Autism Spectrum Disorder, Gray Matter Volume, Cortical Thickness, Total Intracranial Volume, CAT12, FreeSurfer

DOI: 10.22037/IJCN.V18i1.43294

Introduction

Autism Spectrum Disorder (ASD) is a group of neurodevelopmental disorders affecting an individual's perception and interaction, resulting in difficulties in social interaction and communication (1). This disorder encompasses various etiologies and clinical manifestations characterized by repetitive behavior patterns, limited language development, and restricted interests (2). The World Health Organization (WHO) reports a global prevalence of 6.25 cases of ASD per 1,000 individuals (3). Given the increasing prevalence of this disorder, effective treatment strategies are paramount. The term "spectrum disorders" refers to the significant variation in clinical and genetic heterogeneity among people with autism that has hampered the diagnosis and treatment process (4). Typically, ASD is diagnosed when symptoms become severe, and patients experience enduring complications. Consequently, early and accurate diagnosis of ASD is critical (5). Biomarkers are necessary to improve diagnostic accuracy in cases involving unexplained behavioral symptoms (6, 7). Additionally, identifying infants and young children at risk for ASD prior to the onset of behavioral symptoms is essential (8).

Structural Magnetic Resonance Imaging (sMRI), a well-established imaging technique, provides high-resolution anatomical measurements of the brain in the early detection of neurological disorders (9, 10). Besides, numerous studies have employed sMRI to examine anatomical changes in ASD. In recent decades, several studies have examined structural changes in the brains of autistic people and have shown that these changes are associated with ASD (11). According to prevailing theories, total brain volume in individuals with ASD increases rapidly during the first few years of life (12, 13). Moreover, this volume increase tends to be more pronounced in younger patients (14, 15). Morphological research conducted by Riddle et al. suggested that the increase in total brain volume may stem from regional increases in Gray Matter Volume (GMV) rather than white matter (13). Some studies using a Region of Interest (ROI) approach have reported conflicting results of GMV change. Their analysis has shown specific regions with a more significant increment, such as the temporal lobe (16-18), and some regions with a combination of reduction and increases of GMV (19, 20). Conversely, Haar et al. failed to observe volumetric differences in regional gray matter (21).

For nearly three decades, researchers have explored the relationship between the autistic phenotype and changes in Cortical Thickness (CT) (22). There have been notable disputes over advancing CT trajectories in ASD (23). Jiao et al. reported both decreased (in the frontal pole and Parahippocampal gyrus) and increased (in the precuneus and anterior cingulate cortex) cortical thickening in children with ASD aged between 6 and 15 years (24). Khundrakpamet et al.'s research utilizing the Autism Brain Imaging Data Exchange I (ABIDE I) database showed higher CT in frontoparietal areas in individuals with ASD until adolescence (25). Recently, in one study, Nunes et al. considered age-related cortical changes across the entire age range and found no overall group variations in cortical thickness. The group of ASD and Typically Developing (TD) differed in age-related changes, particularly within the frontal and tempo-parietal regions (23).

Evaluation of features such as total brain volume, gray matter volume, and CT can provide valuable insights into the brain's neural structure in healthy individuals and those with autism (26, 27). Methods for evaluating these features can be broadly categorized as surface-based or volume-based. FreeSurfer (FS) is the preferred software for surface-based measurements, while the Computational Anatomy Toolbox (CAT12) is employed for volume-based measurements (28, 29). Volume-based methods reduced processing times, while surface-based approaches outshine accuracy by modeling the entire surface(30). Overall, FS is considered the "gold standard" based on various post-mortem data. This study attempts to find an alternative method that allows images to be processed in less time with comparable accuracy because most neural imaging studies do not require extensive surface reconstruction (24, 31). CAT12 leads to a drastic reduction in processing time due to not using extensive surface reconstruction. Therefore, notably, although FS is more accurate than cat12, the latter provides comparable accuracy in a shorter time and might be considered an alternative to FS (30).

Since the leading cause of many symptoms of ASD is due to changes in the structure of different brain regions, the importance of examining brain structural abnormalities in these children becomes apparent. Therefore, this research aims to initially investigate the differences in CT, GMV, Total Gray Matter (TGM), and Total Intracranial Volume (TIV) features between two groups of ASD and Typically Developing Controls (TDCs) separately for each brain region. Furthermore, it compares surface-based and volume-based CT measurements in FS and CAT12 for both healthy and autism groups. Lastly, the study aims to assess the concordance between these two methods.

Materials & Methods

Participants

The structural sMRI used in this study are taken from the ABIDE II database selected from a data source called NYU Langone Medical Center: Samples Site 1,2 (NYU). More details about the dataset are available at: http://fcon_1000.projects.nitrc.org/indi/abide/. Accurately diagnosing ASD during early childhood is crucial. In this context, this study focused on participants aged five to ten years. Participants were 58 males: 41 with ASD and 18 withTDCs.

Full-scale Intelligence Quotient (FIQ) is a test measuring overall visuospatial intellectual and verbal abilities in human beings, divided into two categories: Performance Intelligence Quotient (PIQ) and Verbal Intelligence Quotient (VIQ). PIQ measures non-verbal capabilities, while VIQ measures the ability to use language for acquiring knowledge and reasoning (32). The Social Responsiveness Scale (SRS) is one of the clinical assessments of autism spectrum disorder, a specific quantitative measure for autistic patients between the ages of 4 and 18 years (33).

MRI Data Acquisition

Brain structural imaging data were prepared using a Siemens MRI 3.0T scanner. Anatomical images were taken using a T1-weighted 3D Turbo Field Echo (TFE) sequence: repetition time and echo time=3.25 ms, acquisition time=8:07 min, flip angle= 7°, slice thickness = 1.3 mm with 0.665 mm gap, plane resolution=1.3 mm×1 mm, 128 slices, the field of view= 256 mm × 256 mm.

Data processing

FreeSurfer processing

The structural MRI data of all participants to estimate cortical thickness and gray matter volume were preprocessed by FS (http://surfer.nmr.mgh.harvard.edu/, version 6.0). FS is an open-source software that processes brain MR images and cortical reconstruction by the recon-all pipeline commonly used in pediatric neuroimaging using default parameters. In the preprocessing stage, the image quality is improved for subsequent processing to improve its execution, increasing processing speed and making it a more convenient procedure. Several steps, including removing the skull, noise, and bias field correction, are performed during this stage, depending on the processing type (Figure 1). The following steps are reconstruction sequences: (1) transferring raw image data voxels to isotropic space, (2) image normalization to estimate and eliminate the bias field, (3) skull stripping, (4) the stages of automatic subcortical segmentation, (5) white matter segmentation, and (6) tessellation of the gray matter–white matter interface (34, 35). (Figure 1)

CAT12 processing

In addition, images were processed using default settings CAT12 toolbox (http://www.neuro.uni-jena.de/cat/, version r1450) and SPM12 (http://www.fil.ion.ucl.ac.uk/spm/software/spm12/, version 7219) in matrix laboratory (MATLAB). This study performed the preprocessing and segmentation steps using CAT12 toolboxes with the default setting. Briefly, all 3D T1-weighted MRI scans were normalized using an affine followed by non-linear registration, corrected for bias field inhomogeneities, and then segmented into GM, WM, and CSF components (36). For this procedure, we used the Diffeomorphic Anatomic Registration Through Exponentiated Lie algebra algorithm (DARTEL) to normalize the segmented scans into a standard MNI space (Figure 2) (37). Volumes were segmented using volume and thickness estimation for ROI analysis. CT and the central surface were measured in one step using a fully automated Projection-Based Thickness (PBT) method. The volume-based algorithm has an acceptable quality compared to surface-based methods and may be superior to existing surface-based approaches in certain respects, such as

reduced processing time (30, 38).

The following steps for surface reconstruction were performed in one step using CAT12 toolbox estimation of cerebral cortex thickness and central surface using a fully automated method that allows for the measurement of cortical thickness and reconstruction of the central surface. It uses tissue segmentation to estimate the White Matter (WM) distance, then projects the local maxima (equal to the cortical thickness) to other gray matter voxels using a neighbor relationship described by the WM distance. The topological correction was performed to repair topological defects using spherical harmonics that allow direct correction of defects on the brain surface mesh (39, 40).

(Figure 2)

ROI extraction

The mean CT, and GMV values for the 68 defined ROIs were calculated using standard methods for ROI extraction provided with software from both the Desikan-Killiany (DK) Atlas (41) and hammers atlas, respectively. These mean values were measured for each ROI in the right and left hemispheres of the brain. Then, the data were entered into SPSS for analysis and statistical models (IBM SPSS Statistics 26).

Hammers Atlas

CAT12 features several volume-based atlases, including the Hammers atlas, which divides the brain into 68 regions—34 per hemisphere. The mean CT value for each ROI was measured separately for the right and left hemispheres (42).

DesikanKilliany Atlas

The Desikan-Killiany atlas (Desikan et al. 2006), well-known in morphometric brain studies, is available in FS6 and CAT12 and thus employed in this study. The cerebral cortex was divided into 68 gyral-based neuroanatomical cortical parcels (34 in each hemisphere). The standard procedures were employed in both methods for extracting the parcel, and the mean CT value for the right and left hemispheres was separately obtained (for each parcel) (43).

Statistical Analysis

Comparison of TDCs and ASDs Using FreeSurfer and CAT12

The normality of these data was assessed using the Kolmogorov-Smirnov test. SPSS 26.0 software was used for statistical analysis. The control and patient group data were separately analyzed with ANCOVA for FS and CAT12 software. First, significant values were extracted from each area. Then, it was examined whether the values obtained from the CAT12 were consistent with the FS method and whether it could be considered a good alternative to FS. The ANCOVA analysis treated age, FIQ, and VIQ as covariates, while the ASD and control groups were the fixed factors. CT and GMV were the dependent variables. Comparison of FS6 and CAT12 Using a TDCs and an ASD

A linear regression model was performed on the TDCs and ASD groups to evaluate the agreement between the ROI estimates of thickness between FS6 and CAT12 software, according to the atlas's definition of the brain structure of healthy individuals. For the analysis, the R2 coefficient of the mean CT values was obtained for all 68 regions between both methods. ANCOVA was used to compare differences in CT estimations between the two methods in TDCs and ASD. Fixed

factors were considered software (FS, CAT12) and constant thickness variable in this model. Bland-Altman diagrams were calculated to further investigate the agreement between CT measured by the two methods. This graphical method shows the difference in estimation between the two approaches. Intra-Class Correlation Coefficients (ICC) were calculated to obtain a simultaneous estimate of compatibility and agreement between CT obtained from the two methods. A value of ICC 1 indicates complete agreement between two (or more) methods, and a value of 0 indicates disagreement.

Results

Demographic and clinical characteristics

In this study, an experimental independents-samples t-test was used to compare groups for age, PIQ, VIQ, Full-Scale Intelligence Quotient (FIQ), and Social Responsiveness Scale (SRS). No significant differences in sex (as all participants were male) or Performance IQ (PIQ) (P = 0.351) were found between the Typically Developing Controls (TDCs) and the Autism Spectrum Disorder (ASD) groups. However, significant differences were noted in age, VIQ, FIQ, and SRS scores, with P-values of 0.002, 0.032, 0.044, and <0.001, respectively. Refer to Table 1 for more information. (Table 1)

Comparison ROIs between TDCs and ASD groups in CAT12 and FS

The mean, standard deviation, and p-value of TIV and total gray matter volume (TGMV) using CAT12 and FS approaches are shown in Tables 2 and 3. According to the p-value between ASD and TDCs groups, no significant difference was observed. (Table 2)

Gray matter volume based on Hammers Atlas at CAT12 in R inferior Middle temporal gyrus, L fusiform gyrus, and R superior frontal gyrus is significantly different (Table 4). Besides, a significant difference between L pars operqularis, R pars operqularis, R pars triangularis, L posterior cingulate, L rostral middle frontal, and R rostral middle frontal according to the DK Atlas in FS was found (Table 5). CT differs significantly in L caudal anterior cingulate, R cuneus, R inferior temporal, and L lateral occipital in CAT12, and L inferior parietal, L lateral occipital, and R pars orbitalis in FS (Table 6).

Comparison of FS6 and CAT12 in the TDCs group

The CT average values of cat12 and FS6 are compared with the t-test, along with their corresponding p-values in Table 6. The R2 coefficient is shown in Table 6, measuring the correlation between the two methods. The minimum and maximum R2 values in the TDCs between CAT12 and FreeSurfer are 0.000 and 0.770, respectively. According to total R2= 0.691 and p-value< 0.001, there was a correlation with moderate regression. The values are shown in Table 6 and Figures 3 and 4.

Comparison of FS6 and CAT12 in the ASD group

The CT average values of cat12 and FS6 are compared with the t-test, along with their corresponding p-values in Table 7. The R2 coefficient is shown in Table 7, measuring the correlation between the two methods. The minimum and maximum R2 values in the ASD between CAT12 and FS are 0.002 and 0.800, respectively. According to total R2=0.680

Table 1: Demographics information for the participants

	ASD (n=40)	TDCs (n=18)	p-value (*)
	Mean (SD)	Mean (SD)	
Age	7.28 (1.29)	8.48(1.43)	0.002*
Sex	40 M	18 M	
FIQ	105.75(18.80)	116.27(15.87)	0.044*
VIQ	107.37(18.35)	118.44(16.29)	0.032*
PIQ	105.92(21.08)	111.22(15.63)	0.3
SRS Total T	74.62(14.30)	44.82(7.13)	

Abbreviations: ASD: Autism Spectrum Disorder; TDCs: typically developing controls; M: Male; FIQ: Full-Scale Intelligence Quotient. PIQ: Performance Intelligence Quotient. VIQ: Verbal Intelligence Quotient. SRS: Social Responsiveness Scale. P< 0.05 was considered statistically significant.

Table 2: Comparison TIV and TGM (mm3) values of TDCs and an ASD Using CAT12 and FreeSurfer 6 (FS6)

Method	Variable	ASD		TDCs		F-value	p-value*
		Mean	SD	Mean	SD		
CAT12	TIV	1448056.75	105856.96	1474817.78	118920.47	0.004	0.949
	TGM	836.27	55.33	829.35	60.93	0.146	0.704
FS6	TIV	1452336.42	127464.53	1480859.12	121724.99	0.003	0.955
	TGM	600.25	45.52	597.12	44.97	0.487	0.488

Abbreviations: ASD: Autism Spectrum Disorder; TDCs: typically developing controls; SD: Standard Deviation; TIV: Total Intracranial Volume; TGM: Total Gray Matter; P< 0.05 was considered statistically significant. (*ANCOVA)

Table 3: Statistical results of Gray Matter volume(mm3) in Hammers Atlas (CAT12)

Brain Region	ASD		TDCs		Mean Difference	F-value	p-value*
	Mean	SD	Mean	SD			
R inferior Middle temporal gyrus	8.71	0.58	8.19	0.39	0.52	8.207	0.006
L fusiform gyrus	2.51	0.22	2.35	0.20	0.16	6.201	0.016
R superior frontal gyrus	28.46	1.91	26.69	1.85	1.77	4.764	0.030

Abbreviations: R: Right; L: Left; ASD: Autism Spectrum Disorder; TDCs: typically developing controls; SD: Standard Deviation; P< 0.05 was considered statistically significant. (*ANCOVA)

Table 4: Statistical results of Gray Matter volume(mm3) in DK Atlas regions (FS6)

Brain Region	ASD		TDCs		Mean Difference	F-value	p-value*
	Mean	SD	Mean	SD			
L pars operqularis	4.06	0.57	3.70	0.52	0.36	4.047	0.049
R pars operqularis	3.33	0.44	3.21	0.39	0.12	3.827	0.036
R pars triangularis	4.03	0.60	3.82	0.62	0.21	4.196	0.035
L posterior cingulate	2.82	0.35	2.54	0.28	0.28	6.926	0.011
L rostral middle frontal	15.93	1.61	14.76	1.71	1.17	6.564	0.013
R rostral middle frontal	16.05	1.55	14.80	0.31	1.25	4.255	0.044

Abbreviations: R: Right; L: Left; ASD: Autism Spectrum Disorder; TDCs: typically developing controls; SD: Standard Deviation; P< 0.05 was considered statistically significant. (*ANCOVA)

Table 5: Statistical results of CT (mm) in DK Atlas regions

Method	Brain Region	ASD		TDCs		Mean Difference	F-value	p-value*
		Mean	SD	Mean	SD			
CAT12	L caudal anterior cingulate	1.69	0.19	1.54	0.21	0.15	5.557	0.022
	R cuneus	1.53	0.15	1.54	0.16	-0.01	4.370	0.041
	R inferior temporal	1.91	0.14	1.86	0.17	0.05	4.523	0.031
	L lateral occipital	1.59	0.12	1.53	0.14	0.06	4.149	0.047
FS6	L inferior parietal	1.97	0.22	1.87	0.17	0.10	5.317	0.025
	L lateral occipital	1.69	0.20	1.58	0.16	0.11	5.412	0.024
	R pars orbitalis	2.27	0.29	2.11	0.29	0.16	4.289	0.043

Abbreviations: R: Right; L: Left; ASD: Autism Spectrum Disorder; TDCs: typically developing controls; SD: Standard Deviation; P< 0.05 was considered statistically significant. (*ANCOVA)

Table 6: Comparison means values of CT (mm) Both Methods Including TDCs Subjects

Brain Region	FS6		CAT12		p-value	R2
	Mean	SD	Mean	SD		
L banks of superior temporal sulcus	2.71	0.14	2.98	0.29	0.009	0.360
R banks of superior temporal sulcus	2.89	0.19	3.08	0.20	0.066	0.200
L caudal anterior cingulate	2.75	0.31	2.73	0.37	0.181	0.110
R caudal anterior cingulate	2.53	0.12	2.82	0.35	0.528	0.030
L caudal middle frontal	2.90	0.11	3.32	0.14	<0.001	0.580
R caudal middle frontal	2.88	0.14	3.33	0.17	0.001	0.520
L cuneus	2.26	0.15	2.58	0.19	<0.001	0.550
R cuneus	2.29	0.16	2.62	0.23	0.001	0.540
L entorhinal	3.43	0.25	4.76	0.50	0.122	0.140
R entorhinal	3.62	0.10	4.86	0.45	0.965	0.000
L fusiform	2.83	0.11	3.32	0.20	<0.001	0.570
R fusiform	2.91	0.13	3.38	0.17	0.029	0.270
L inferior parietal	2.75	0.10	3.18	0.18	<0.001	0.650
R inferior parietal	2.77	0.08	315	0.16	0.001	0.540
L inferior temporal	2.94	0.12	3.51	0.19	0.001	0.510
R inferior temporal	3.01	0.10	3.54	0.17	<0.001	0.580
L isthmus cingulate	2.49	0.14	3.34	0.12	0.658	0.010
R isthmus cingulate	2.47	0.20	3.24	0.27	0.144	0.130
L lateral occipital	2.33	0.12	2.63	0.16	<0.001	0.740
R lateral occipital	2.43	0.12	2.67	0.17	<0.001	0.740
L lateral orbitofrontal	3.14	0.19	3.84	0.23	0.017	0.310
R lateral orbitofrontal	3.07	0.18	3.86	0.24	0.155	0.120
L lingual	2.45	0.15	2.67	0.14	0.946	0.000
R lingual	2.41	0.13	2.79	0.27	0.039	0.240
L medial orbitofrontal	2.74	0.10	3.24	0.19	0.070	0.190
R medial orbitofrontal	2.80	0.13	3.18	0.15	0.019	0.300
L middle temporal	3.10	0.13	3.82	0.20	0.020	0.300
R middle temporal	3.13	0.12	3.81	0.20	0.006	0.390

L parahippocampal	2.75	0.20	3.05	0.24	0.596	0.020
R parahippocampal	2.75	0.20	3.24	0.24	0.838	0.000
L paracentral	2.85	0.14	3.06	0.17	<0.001	0.650
R paracentral	2.92	0.14	3.11	0.16	0.072	0.190
L pars opercularis	2.91	0.13	3.36	0.20	0.016	0.310
R pars opercularis	2.91	0.13	3.35	0.27	0.002	0.470
L pars orbitalis	3.17	0.21	3.88	0.28	<0.001	0.570
R pars orbitalis	3.09	0.24	3.85	0.27	0.019	0.300
L pars triangularis	2.91	0.13	3.29	0.28	0.007	0.370
R pars triangularis	2.91	0.14	3.34	0.27	0.004	0.420
L pericalcarine	1.99	0.21	2.39	0.21	0.001	0.520
R pericalcarine	1.99	0.15	2.43	0.21	0.020	0.300
L postcentral	2.36	0.11	2.69	0.13	<0.001	0.740
R postcentral	2.34	0.12	2.74	0.18	0.001	0.480
L posterior cingulate	2.56	0.14	2.87	0.20	0.002	0.460
R posterior cingulate	2.57	0.14	2.94	0.21	0.052	0.220
L precentral	2.80	0.07	3.03	0.13	0.003	0.440
R precentral	2.77	0.08	2.99	0.10	0.184	0.110
L precuneus	2.78	0.06	3.19	0.16	0.029	0.260
R precuneus	2.80	0.08	3.25	0.13	0.011	0.340
L rostral anterior cingulate	2.90	0.20	3.18	0.23	0.019	0.300
R rostral anterior cingulate	2.82	0.20	3.26	0.26	0.013	0.330
L rostral middle frontal	2.85	0.14	3.36	0.20	<0.001	0.720
R rostral middle frontal	2.81	0.14	3.31	0.19	0.001	0.530
Superior frontal L	3.15	0.16	3.57	0.20	<0.001	0.770
R superior frontal	3.14	0.13	3.58	0.18	<0.001	0.650
L superior parietal	2.57	0.08	2.80	0.10	<0.001	0.640
R superior parietal	2.54	0.09	2.78	0.08	0.011	0.340
L superior temporal	3.04	0.09	3.39	0.14	0.222	0.090
R superior temporal	3.14	0.10	3.54	0.18	<0.001	0.650
L supramarginal	2.89	0.10	3.23	0.16	0.008	0.360
R supramarginal	2.87	0.06	3.12	0.14	0.001	0.500
L frontal pole	3.14	0.22	3.56	0.32	0.293	0.070
R frontal pole	3.15	0.31	3.67	0.35	0.004	0.410
L temporal pole	3.64	0.24	4.48	0.43	0.350	0.060
R temporal pole	3.63	0.36	4.58	0.48	0.371	0.050
L transverse temporal	2.76	0.22	3.05	0.19	0.729	0.010
R transverse temporal	2.78	0.25	3.03	0.31	0.348	0.060
L insula	3.11	0.16	3.97	0.21	0.687	0.010
R insula	3.11	0.09	4.13	0.28	0.470	0.030
Total	2.83	0.37	3.29	0.56	<0.001	0.690

Abbreviations: R: Right; L: Left; ASD: Autism Spectrum Disorder; TDCs: typically developing controls; SD: Standard Deviation; R2: Regression; $P< 0.05$ was considered statistically significant.

Table 7: Comparison means values of CT (mm) Both Methods Including ASD Subjects

Brain Region	FS6		CAT12		p-value	R2
	Mean	SD	Mean	SD		
L banks of superior temporal sulcus	2.78	0.17	3.01	0.26	<0.001	0.450
R banks of superior temporal sulcus	2.84	0.16	3.11	0.24	0.001	0.260
L caudal anterior cingulate	2.70	0.22	2.93	0.35	0.006	0.190
R caudal anterior cingulate	2.55	0.17	2.90	0.29	0.187	0.050
L caudal middle frontal	2.93	0.11	3.33	0.14	<0.001	0.370
R caudal middle frontal	2.91	0.12	3.35	0.14	<0.001	0.320
L cuneus	2.31	0.22	2.62	0.23	<0.001	0.430
R cuneus	2.32	0.20	2.61	0.23	<0.001	0.650
L entorhinal	3.47	0.30	5.02	0.45	0.168	0.050
R entorhinal	3.50	0.34	5.09	0.40	0.768	0.002
L fusiform	2.86	0.16	3.40	0.24	<0.001	0.350
R fusiform	2.89	0.11	3.45	0.22	0.001	0.250
L inferior parietal	2.82	0.10	3.25	0.15	<0.001	0.380
R inferior parietal	2.81	0.09	3.24	0.15	<0.001	0.380
L inferior temporal	3.01	0.19	3.65	0.21	0.001	0.260
R inferior temporal	3.10	0.15	3.75	0.25	0.002	0.240
L isthmus cingulate	2.49	0.14	3.35	0.32	0.173	0.050
R isthmus cingulate	2.52	0.20	3.27	0.29	0.030	0.120
L lateral occipital	2.43	0.13	2.74	0.18	<0.001	0.350
R lateral occipital	2.49	0.13	2.77	0.19	<0.001	0.580
L lateral orbitofrontal	3.14	0.15	3.88	0.26	<0.001	0.350
R lateral orbitofrontal	3.05	0.14	3.92	0.27	<0.001	0.410
L lingual	2.50	0.17	2.79	0.20	0.007	0.180
R lingual	2.49	0.14	2.82	0.22	0.510	0.010
L medial orbitofrontal	2.81	0.18	3.35	0.25	<0.001	0.330
R medial orbitofrontal	2.81	0.19	3.25	0.20	0.001	0.250
L middle temporal	3.10	0.11	3.85	0.24	0.002	0.230
R middle temporal	3.17	0.16	3.93	0.22	0.677	0.005
L parahippocampal	2.84	0.21	3.11	0.29	0.005	0.200
R parahippocampal	2.69	0.20	3.16	0.25	0.005	0.200
L paracentral	2.89	0.13	3.12	0.19	<0.001	0.380
R paracentral	2.86	0.14	3.10	0.20	<0.001	0.350
L pars opercularis	2.90	0.14	3.35	0.22	<0.001	0.440
R pars opercularis	2.88	0.12	3.34	0.21	0.053	0.100
L pars orbitalis	3.27	0.19	3.99	0.31	0.014	0.150
R pars orbitalis	3.25	0.17	3.99	0.32	<0.001	0.360
L pars triangularis	2.92	0.15	3.25	0.24	0.030	0.120
R pars triangularis	2.95	0.16	3.40	0.26	<0.001	0.290
L pericalcarine	2.11	0.25	2.49	0.24	<0.001	0.520
R pericalcarine	2.05	0.18	2.47	0.23	<0.001	0.440
L postcentral	2.38	0.14	2.75	0.16	<0.001	0.630
R postcentral	2.34	0.12	2.77	0.15	<0.001	0.520

Brain Region	FS6		CAT12		p-value	R2
	Mean	SD	Mean	SD		
L posterior cingulate	2.62	0.17	2.99	0.22	0.001	0.270
R posterior cingulate	2.53	0.15	2.95	0.23	<0.001	0.510
L precentral	2.80	0.09	3.03	0.11	<0.001	0.450
R precentral	2.77	0.11	3.00	0.13	<0.001	0.430
L precuneus	2.80	0.13	3.24	0.18	<0.001	0.640
R precuneus	2.81	0.10	3.28	0.17	<0.001	0.630
L rostral anterior cingulate	2.86	0.19	3.31	0.36	0.060	0.090
R rostral anterior cingulate	2.90	0.25	3.37	0.31	0.003	0.210
L rostral middle frontal	2.91	0.11	3.46	0.21	<0.001	0.570
R rostral middle frontal	2.88	0.11	3.43	0.20	<0.001	0.540
L Superior frontal	3.16	0.09	3.59	0.16	<0.001	0.460
R superior frontal	3.13	0.11	3.63	0.15	<0.001	0.490
L superior parietal	2.60	0.12	2.85	0.16	<0.001	0.800
R superior parietal	2.58	0.13	2.83	0.17	<0.001	0.760
L superior temporal	3.08	0.13	3.43	0.18	<0.001	0.420
R superior temporal	3.14	0.13	3.63	0.21	<0.001	0.550
L supramarginal	2.91	0.12	3.27	0.19	<0.001	0.520
R supramarginal	2.90	0.11	3.23	0.18	<0.001	0.400
L frontal pole	3.29	0.27	3.78	0.36	0.037	0.110
R frontal pole	3.30	0.26	3.74	0.38	<0.001	0.340
L temporal pole	3.65	0.32	4.54	0.38	0.366	0.020
R temporal pole	3.69	0.30	4.75	0.41	0.007	0.180
L transverse temporal	2.79	0.22	3.19	0.37	0.002	0.230
R transverse temporal	2.83	0.23	3.18	0.37	0.335	0.030
L insula	3.13	0.16	4.01	0.34	<0.001	0.290
R insula	3.08	0.17	4.17	0.35	<0.001	0.330
Total	2.86	0.37	3.36	0.59	<0.001	0.680

Abbreviations: R: Right; L: Left; ASD: Autism Spectrum Disorder; TDCs: typically developing controls; SD: Standard Deviation; R2: Regression; $P< 0.05$ was considered statistically significant.

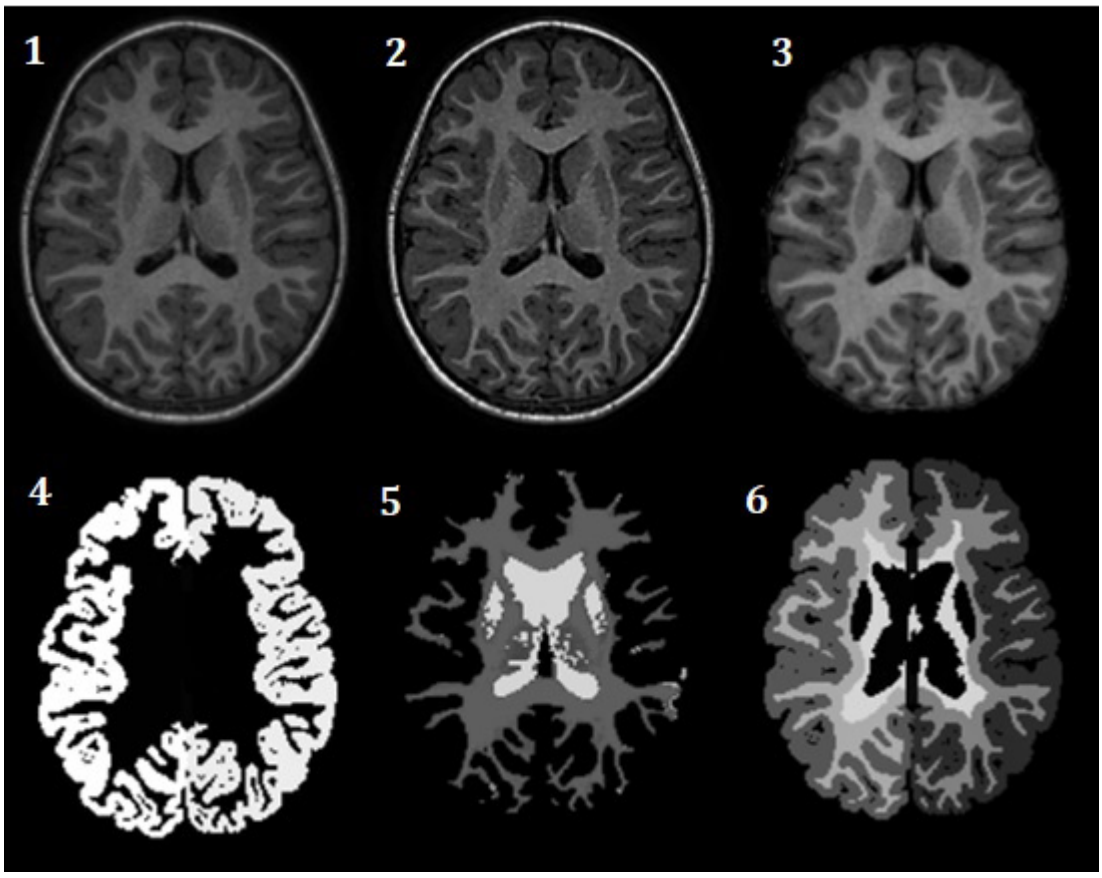

Figure 1. *Steps 1 to 6 of FreeSurfer MRI reconstruction*

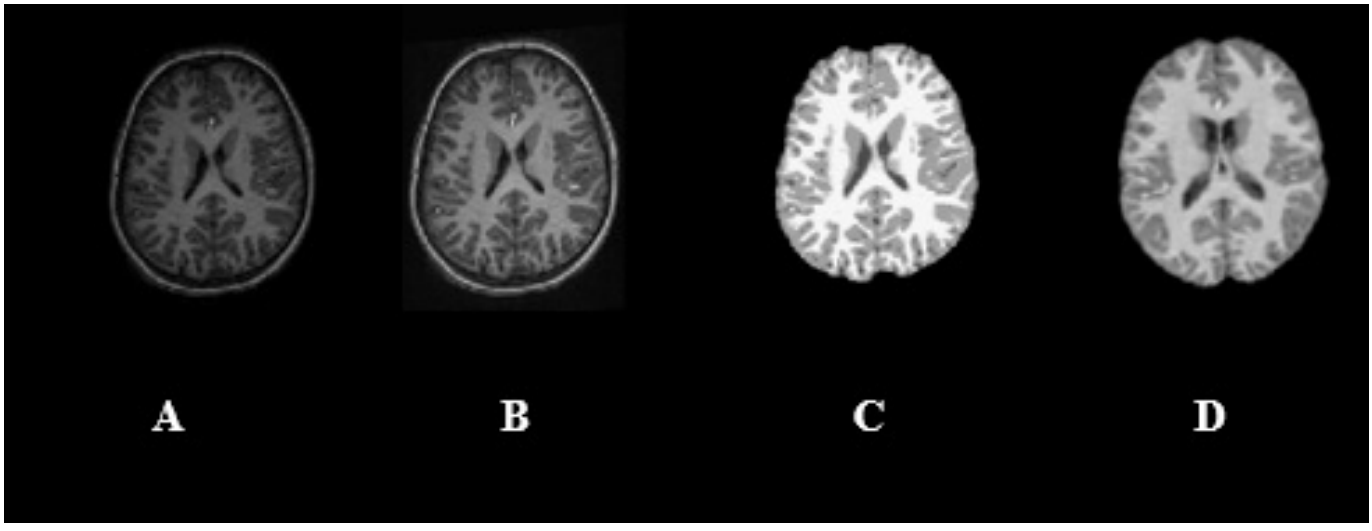

Figure 2. *Stages of pre-processing of structural images of the brain: A) Initial image, B) Image after intensity normalization, C) Segmented image with skull removal, and D) Image after spatial normalization in DARTEL modified space based on MNI.*

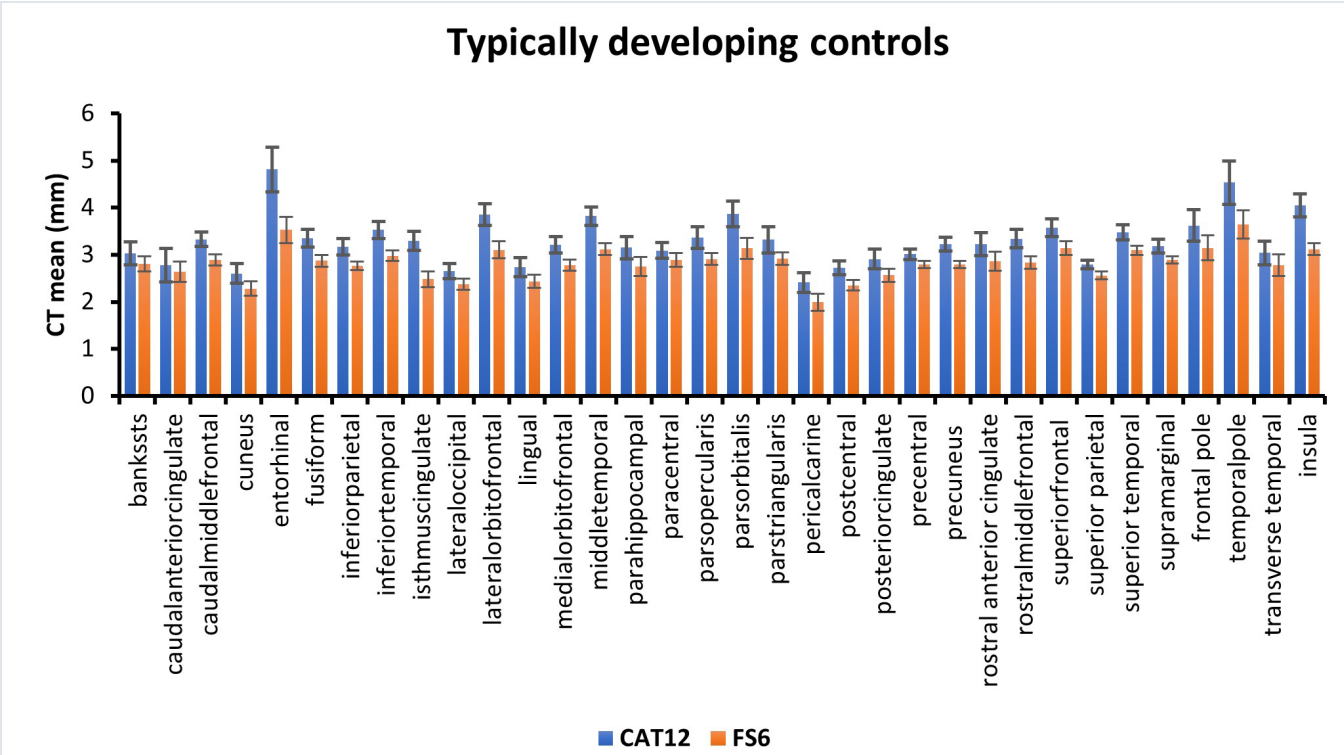

Figure 3. *Mean CT values for 34 Regions of Interest (ROI) of FreeSurfer (FS6) and CAT12 (TDCs).*

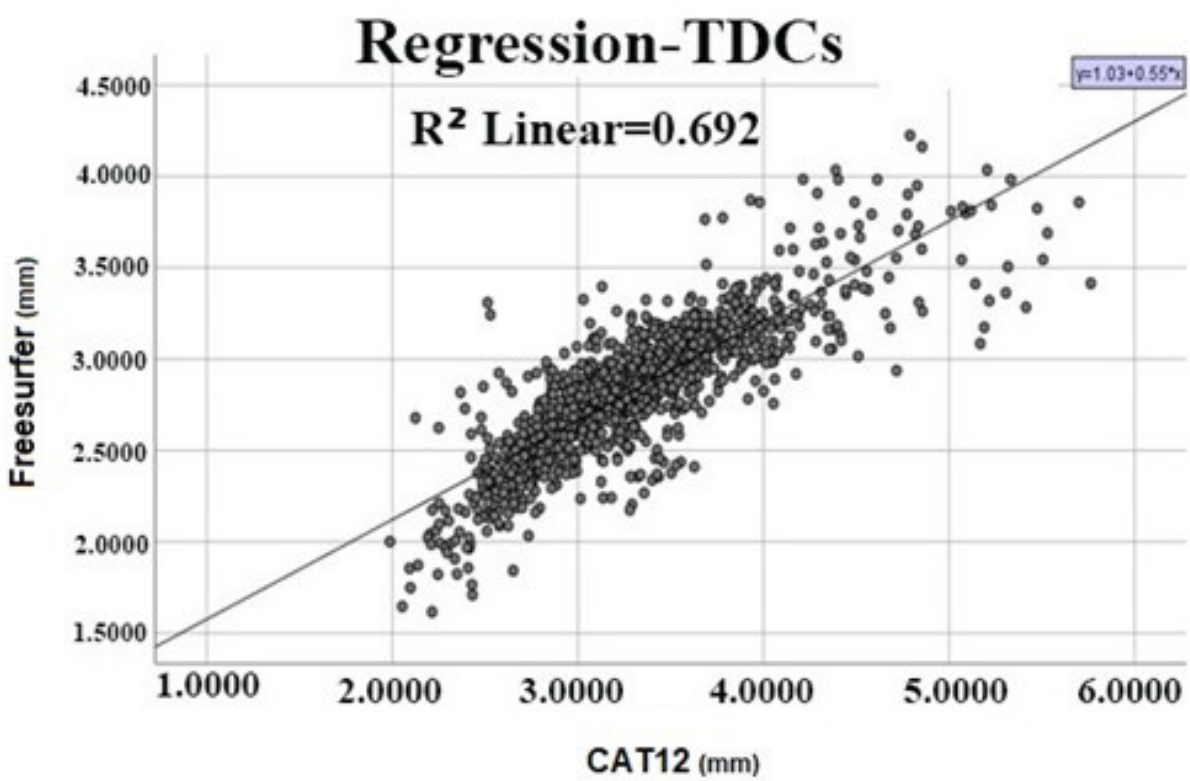

Figure 4. *Regression between CT outcomes in the TDCs using CAT12 and FreeSurfer methods.*

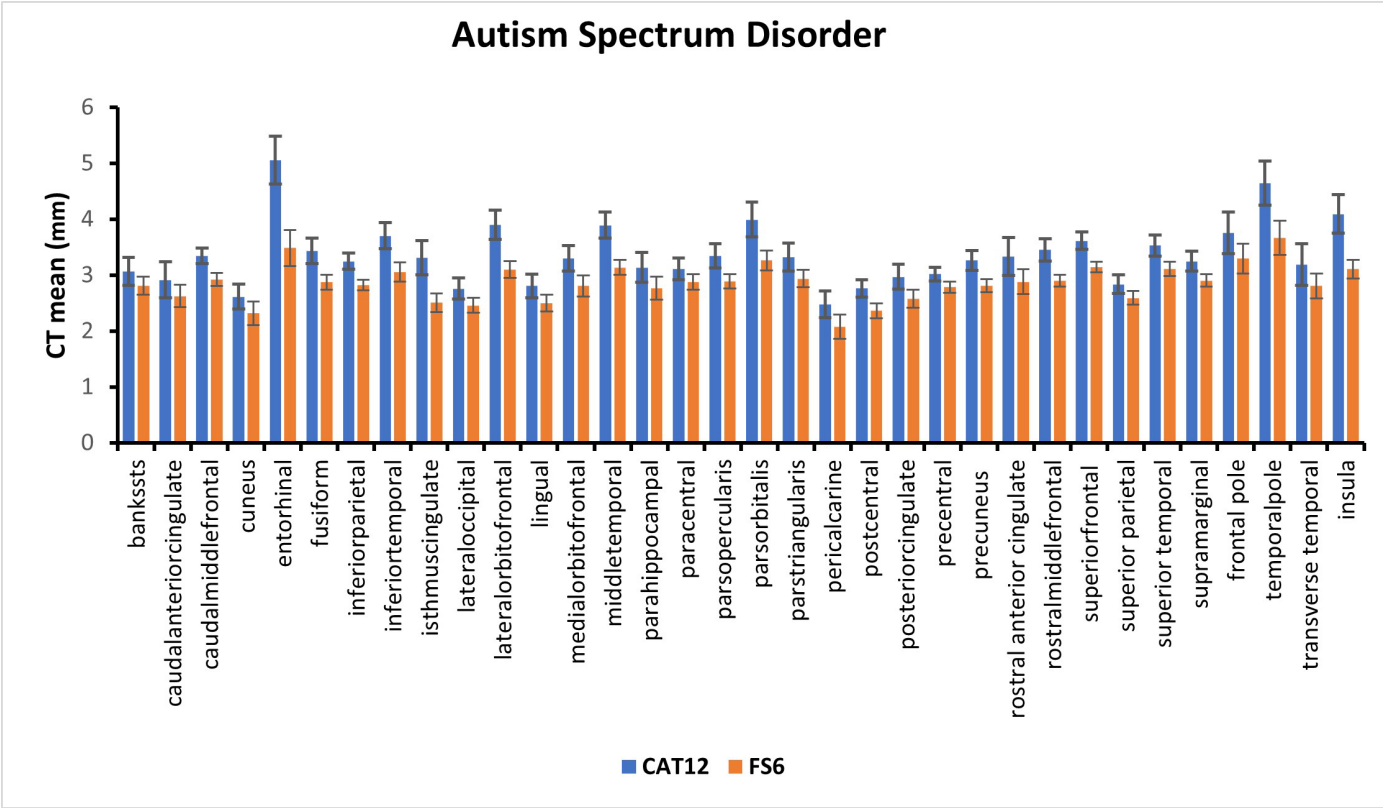

Figure 5. *Mean CT values for 34 regions of interest (ROI) of FreeSurfer (FS6) and CAT12 (ASD).*

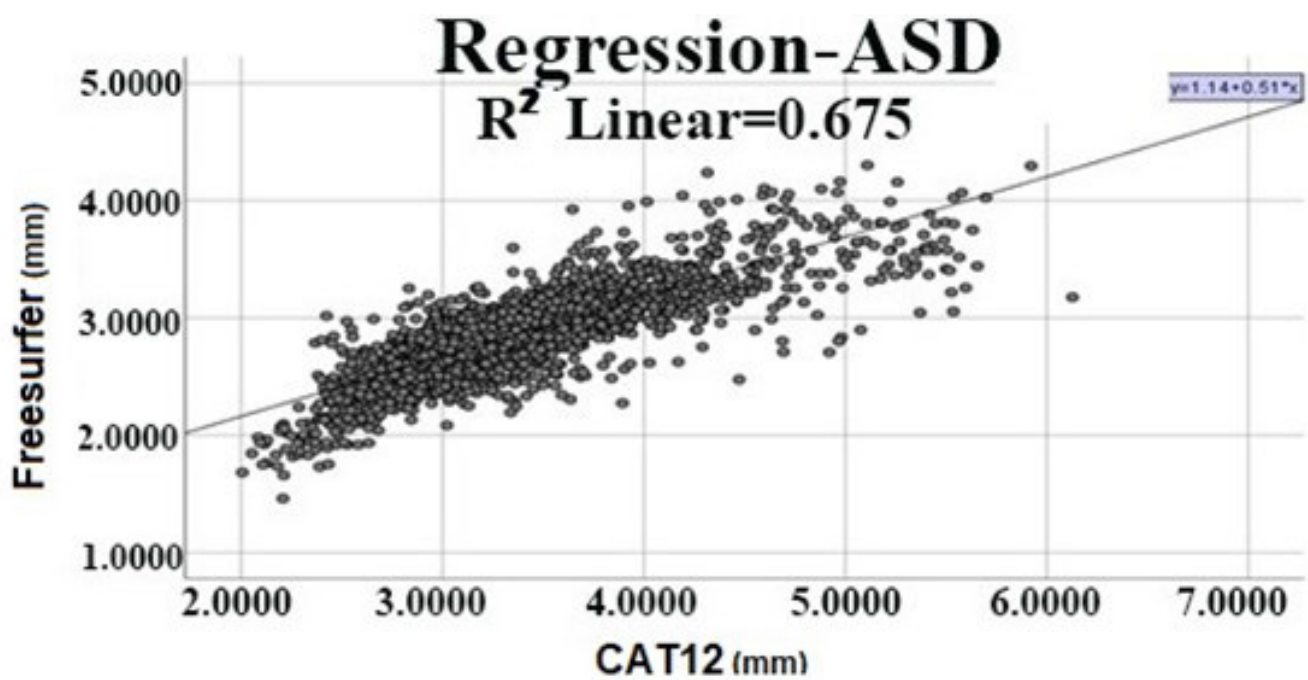

Figure 6. *Regression between CT outcomes in the ASD using CAT12 and FreeSurfer methods.*

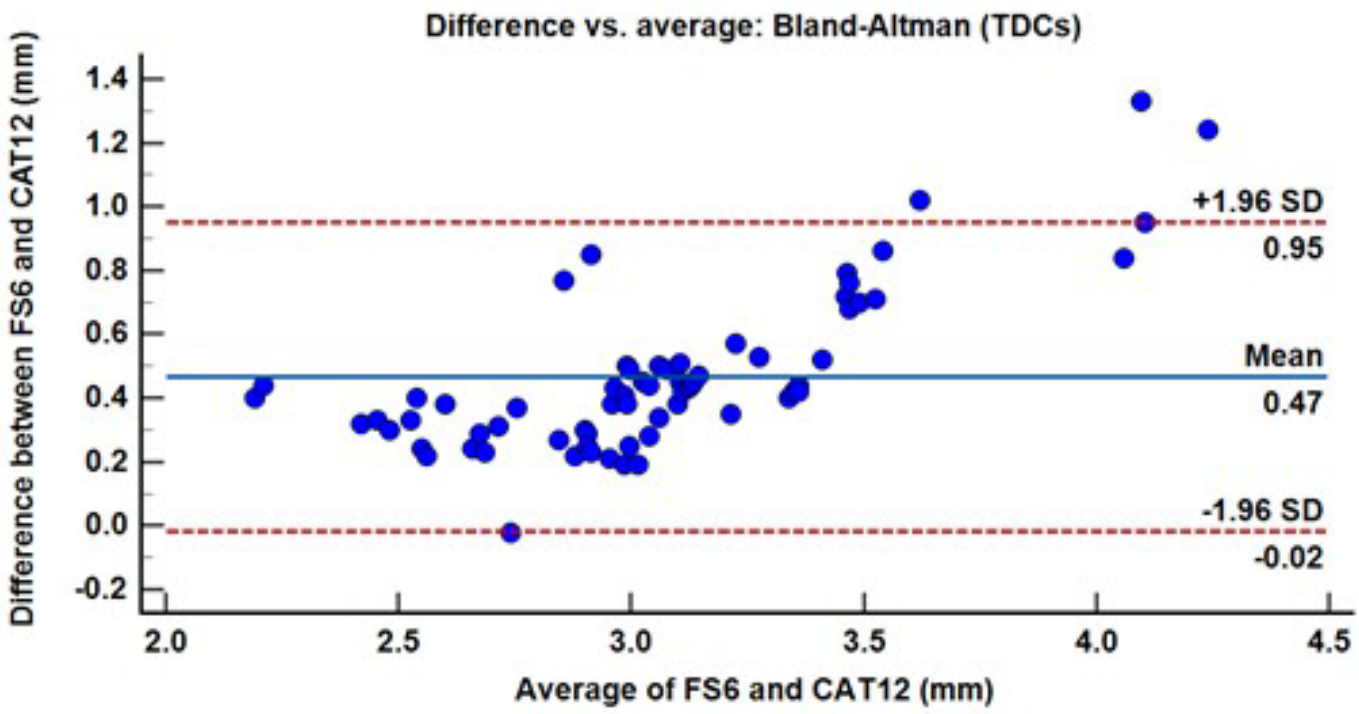

Figure 7. *Bland-Altman chart with agreement limits (dotted lines) for average CT values TDCs group.*

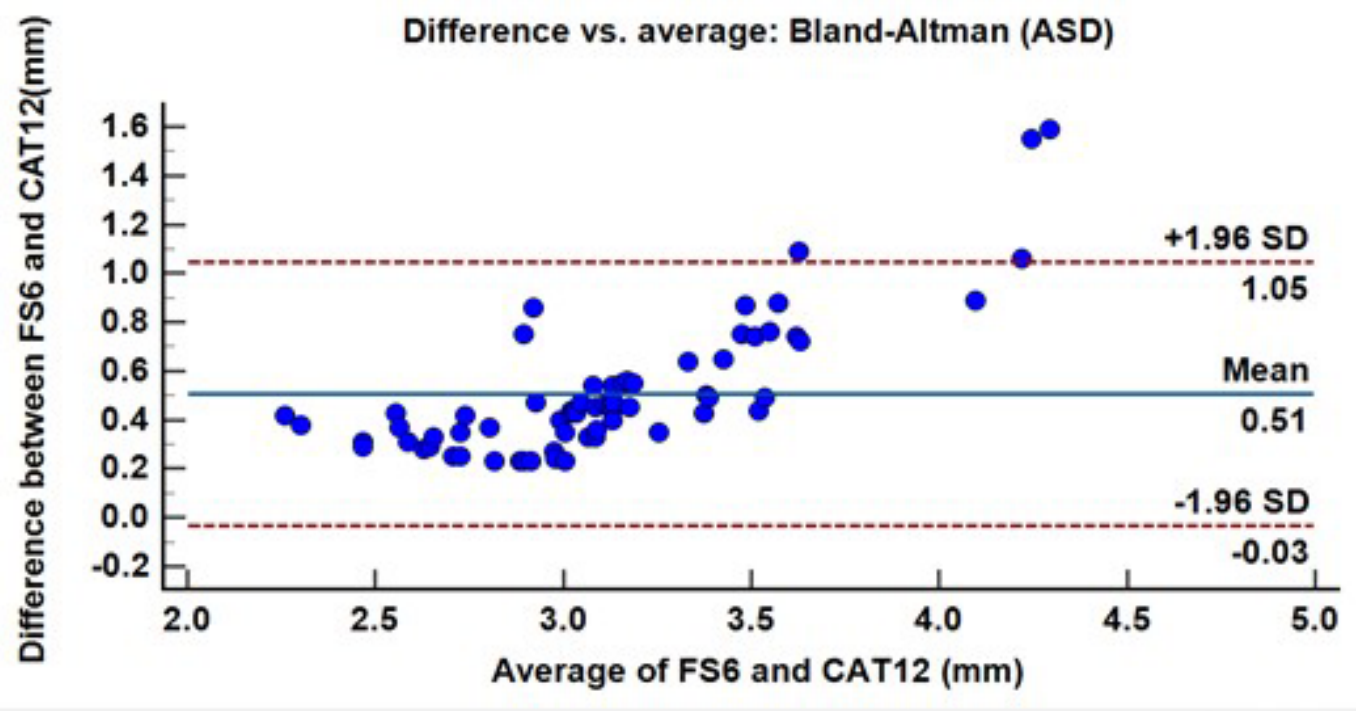

Figure 8. *Bland-Altman chart with agreement limits (dotted lines) for average CT values ASD group.*

and p-value < 0.001, there was a correlation with moderate regression. The values are seen in Table 7 and Figures 5 and 6.

According to the Bland-Altman chart, overall CT values were higher for CAT12. The differences between the two methods were greater at higher thickness values, particularly in the ASD group. See Figures 7 and 8 for more details. Based on the results of ICC analysis, Cronbach's alpha coefficient for the TDCs and ASD groups was 0.865 and 0.848, respectively, and the F-test value for both groups was < 0.001.

Discussion

The following evaluations were performed the present study using the CAT12 volume-based toolbox for SPM and FS6 surface-based. Firstly, overall differences in GMV, CT, TGM, and TIV between the autistic and healthy groups were separately compared for each method. Subsequently, the regression analysis was performed for CT values and volume of TGM and TIV in both FS and CAT12 methods. Additionally, the agreement between the two methods was evaluated through the Bland-Altman and ICC to determine the potential of CAT12 software as an alternative to FS. In this statistical analysis, age, VIQ, and FIQ were considered covariates due to significant differences between the healthy and autism groups. The inclusion of these variables, particularly age, was expected based on previous studies (44-46), which have highlighted the influence of these factors on brain structure, such as total brain GM volume and CT (47, 48).

According to the statistical findings presented in Tables 2 and 3, there were no significant differences in TIV and TGM between individuals with ASD and TDCs. These findings contradict several past studies (49-51). However, similar to the obtained results, Xiao et al. reported a need for significant differences (52, 53). Summing the total volume of GM, WM, and CSF gives the total intracranial volume (TIV) (TIV = TGM + TWM + TCSF) (51, 54). While investigating the potential of TIV as a biomarker for autism diagnosis is crucial, it should be considered as an auxiliary factor when there is a significant difference in TIV between the healthy and autistic groups. This consideration can lead to more reliable and accurate results (30, 54). In this study, TIV showed no significant differences between the healthy and autistic groups; therefore, we excluded it from the statistical analysis. Based on the values presented in Table 4, the GM volume measured by CAT12 was significantly increased in the R inferior Middle temporal gyrus, L fusiform gyrus, and R superior frontal region of the brain in the autistic group compared to the control group. The social problems in ASD may be due to deficiencies in these regions, indicating their role in cognition and social communication (55-57).

Some studies, including the present study, have reported an increase in GM volume in the right inferior middle temporal gyrus region (58, 59), while others have reported a decrease (44, 60). Foster et al. demonstrated reduced gray matter volume in the left fusiform gyrus (18), whereas previous studies have reported increases in GM volume in both the left fusiform gyrus and right superior frontal region in ASD (61, 62). Wallace et al. found an increase in the left fusiform gyrus and a reduction in the right superior frontal region (62). Differences in GM volume between different age

groups in autism were shown in the Duerden et al. study, increasing GM volume in the left fusiform gyrus reported for children/ adolescents. Uniquely in the fusiform gyrus, there was a significant likelihood of decreased gray matter volume in the adults (19).

The results obtained using the FS approach showed that the GM volume increases in several regions, including the left pars operqularis, right pars operqularis, right pars triangularis, left posterior cingulate, left rostral middle frontal, and right rostral middle frontal. These regions play essential roles in social and language processing as executive tasks. Structural changes in any of these regions could potentially contribute to the development of autism. The pars operqularis, primarily due to its role in the human mirror nervous system (MNS), maybe a reason for social interaction deficiencies in ASD (61, 63, 64).

Knaus et al. has found an increase in GM volume in the pars opercularis and triangularis regions(65). A significant gray matter volume reduction in both the pars opercularis and triangularis bilaterally in the subjects with ASD compared with the typical control subjects was reported by Yamasaki et al. (66). These findings align with the study conducted by McAlonan et al. (67). In this study CT scans were extensively utilized as a sensitive biomarker to assess brain disorders. Two methods based on the Desikan-Killiany atlas were employed for this purpose. Significant differences in CT were observed in the left caudal anterior cingulate, right cuneus, right inferior temporal, and left lateral occipital regions using CAT12, while differences were found in the left inferior parietal, left lateral occipital, and right pars orbitalis regions using FS. In individuals with ASD, compared to TDCs, there was an increase in thickness in all these areas except the right cuneus. The left caudal anterior cingulate and left inferior parietal in the brain are known to play a role in social and cognitive behaviors (68, 69).

The right cuneus and left lateral occipital regions are also involved in the comprehension of visual processing (70, 71). The CT of the right inferior temporal region is generally associated with language and emotional understanding (72). Specifically, the right pars orbitalis, a subdivision of the inferior frontal gyrus, is functionally linked to the recognition of facial expressions depicting basic emotions (73). Research has confirmed an increase in CT in the left caudal anterior cingulate and right inferior temporal regions in individuals with autism compared to controls (24, 74), respectively. In contradiction with the study, several prior reports have shown a reduction in CT in the right inferior temporal (75), left lateral occipital (76), and right pars orbitalis (24) regions. Zielinski et al. observed thicker cortical measurements in the cuneus during childhood in individuals with ASD, which contradicts the obtained findings (22). The inconsistency among previous studies may be attributed to various factors, including differences in data collection, feature extraction methods and software used, discrepancies in IQ, gender, age, clinical characteristics, racial composition, and climatic factors of the samples, as well as small sample sizes. Nevertheless, larger samples are necessary to obtain reliable results (53, 77, 78).

The causes, risk factors, and clinical manifestations of ASD are varied, possibly related to changes in the brain's anatomical neurological abnormalities

(2). ASD has a strong genetic basis, and many ASD-related genes influence the formation of neuronal circuits (79). ASD is associated with a variety of gene mutations, each of which affects nerve growth through various pathways and methods, including gene transcription, expression and regulation, synaptic formation, and function. Cell migration can also vary the clinical manifestations of ASD symptoms (80, 81). For example, Shank/ ProSAP proteins are critical to synaptic formation, function, and development. Strongly, mutations in the SHANK genes and alteration of Shank protein expression lead to abnormal synaptic development and are related to learning and social cognition deficits in ASD (82).

To better understand the relationship between heterogeneous neuropathological phenotypes and the clinical manifestations of ASD, more phenotypic, genetic, and neuroimaging data are required, leading to the discovery of new and effective biomarkers (83). Future studies should aim to use larger sample sizes and establish inclusion criteria based on IQ, gender, age, and diagnosis. The crucial factors influencing the results are the different methods used to process and extract the feature are one of. This study used two approaches based on volume (CAT12) and surface-based (FS6) analyses. Since there is no gold standard for fully automated CT estimation, selecting a method that produces the most accurate results can be challenging. However, post-mortem and histological studies show good agreement between post-mortem measurements and FS CT estimates. As no post-mortem and histological studies are available for CAT12, this study compared CAT12 results with FS results to determine usability (38).

This research aims to compare ROI-wise CT estimations obtained using the CAT12 toolbox and the FS6 software for both the TDCs group and ASD. The CT values calculated by CAT12 were generally higher than those obtained using the FS6 software in all regions except the right cuneus. These findings contrast with the results of some studies (30, 38). The discrepancies between the present findings and those of other studies may stem from various sources. The differences could be attributed to the narrower age range of participants or variations in MRI protocols used for imaging. The software version plays an essential role in obtaining results since it may have implemented various methods, giving rise to different results. Regression, the Bland-Altman graphs, and ICC were used to assess the agreement and correlation between the two software. The results indicated that the regression analysis comparing the mean ROI of CT estimation in the TDCs group yielded slightly higher values than in the ASD group. In both TDCs and ASD groups, there was some link between the two methods, according to the p-value, and considering the value of R2, a moderate correlation was obtained. The ICC analysis confirmed the study hypothesis by demonstrating a significant relationship between the values calculated by the two software, and the obtained alpha coefficient showed relatively good reliability. The Bland-Altman chart illustrated the average agreement between the two applications.

The study by Seiger et al., Which was performed on the elderly with Alzheimer's disease, showed an excellent agreement between the CT estimates obtained from the two methods despite CAT12 yielding higher CT values than FS (30). Similarly,

Masouleh et al. performed thickness estimation using the CAT12 toolbox and FS6 software on large samples of healthy young and old adults, and they achieved excellent agreement between the two methods (84). The CT values obtained from both methods significantly correlate with each other across ROIs and demonstrate that both methods are consistent. Notably, Ay et al. reported that the results can be extracted from both methods for group comparison purposes (38). Pulli et al. reported a relatively weak agreement between the two approaches in a pediatric population of 5-year-olds. (85).

The findings from this study indicate a lower correlation and agreement than the initial two studies and a higher value than the results reported by Pulli et al. This discrepancy could be due to the CAT12 Toolbox potentially overestimating CT values, the smaller sample size in this study relative to others, and the consideration of varying age groups (30, 84, 85). Additionally, there is diversity at different levels of analysis, and differences in analysis pipelines should be considered to estimate thickness. For example, estimates of cerebral cortex thickness, differences in algorithms used for skull stripping or brain extraction, voxel-based initial and final records, and various tissue bias correction and classification algorithms are all likely to be affected (85).

On the other hand, the maximum CT value that FS can calculate is 5 mm. In the present study, about one percent of the CTs are above 5 mm, providing the potential for a ceiling effect in the FS CT values. Nevertheless, considering that, the value of 5 mm for CT was not observed in the data obtained in this study by FS, this effect can be considered insignificant or ignored. Considering the moderate agreement between CAT12 and FS6 approaches for the autistic group of children, it appears that cat12 cannot be universally substituted for FS6 in all conditions.

Limitations

The limitations of the present study include insufficient data, which might decrease the power of the study's statistics: confounding factors, failure to consider experimental artifacts, gender, and intelligence tests. Furthermore, due to the lack of imaging and clinical data on infants, subjects in the age range of 5-10 years were used in both autism and control groups. Those comorbidities with autism, such as epilepsy, can affect both the surface and volume of the brain. The present study has no information about autism-related diseases in selected patients. Therefore, to achieve more credible results due to the variety of ASD clinical phenotypes in future studies, these limitations should be considered. Information on autism and control subjects with younger ages and a larger sample size can be used. In addition, it is better to consider the effects of each processing step on the results of estimating the thickness of the cerebral cortex.

In Conclusion

In this study, sMRI was utilized to identify abnormal brain areas in individuals with ASD. The analysis of gray matter volume based on atlases hammers and DK revealed significant differences between the ASD group and TDCs in certain regions of interest (ROIs). Moreover, abnormalities in CT were observed in the autism group. These findings

suggest that changes in brain structure are closely associated with the clinical features of ASD, which can potentially contribute to early diagnosis. In addition, a moderate level of agreement between the two methods indicates some degree of consistency in the results. In summary, although CAT12 provides some valuable information in investigating ASD in children, the differences are also considerable compared to FS6. To fully understand the accuracy and limitations of these software tools, further studies with larger sample sizes are necessary to account for all influencing factors.

Acknowledgment

This article is taken from the Ph.D. thesis and involving human participants were reviewed and approved by [Research Ethics Committee of School of Medicine- Mashhad University of Medical Sciences]. Since we used pre-prepared data, there is no need for consent statement.
Ethics code: IR.MUMS.MEDICAL.REC.1399.089

Author's Contribution

Reyhane Faraji Summarize articles and extract important points and write the article of this review: Reyhane Faraji and Zohreh Ganji Selecting appropriate articles based on the set criteria, reviewing the written article in terms of writing accuracy: Zahra Khandan Khadem Alreza and Hossein Akbari-Lalimi Graphic design and structural review of the article: Fereshteh Eidy Manuscript writing: All authors Final approval of manuscript: All authors responsible and supervising the scientific accuracy of the content written in this article

Conflict of Interest

The authors report no conflict of interest.

References

1. Baio J, Wiggins L, Christensen DL, Maenner MJ, Daniels J, Warren Z, et al. Prevalence of autism spectrum disorder among children aged 8 years—autism and developmental disabilities monitoring network, 11 sites, United States, 2014. MMWR Surveillance Summaries. 2018;67(6):1.
2. Wasilewska J, Klukowski M. Gastrointestinal symptoms and autism spectrum disorder: links and risks–a possible new overlap syndrome. Pediatric health, medicine and therapeutics. 2015;6:153.
3. Sabbagh HJ, Al-Jabri BA, Alsulami MA, Hashem LA, Aljubour AA, Alamoudi RA. Prevalence and characteristics of autistic children attending autism centres in 2 major cities in Saudi Arabia: A cross-sectional study. Saudi Medical Journal. 2021;42(4):419.
4. Dekhil O, Hajjdiab H, Shalaby A, Ali MT, Ayinde B, Switala A, et al. Using resting state functional mri to build a personalized autism diagnosis system. PloS one. 2018;13(10):e0206351.
5. Akhavan Aghdam M, Sharifi A, Pedram MM. Combination of rs-fMRI and sMRI data to discriminate autism spectrum disorders in young children using deep belief network. Journal of digital imaging. 2018;31(6):895-903.
6. Yerys BE, Pennington BF. How do we establish a biological marker for a behaviorally defined disorder? Autism as a test case. Wiley Online Library; 2011. p. 239-41.
7. Frye RE, Vassall S, Kaur G, Lewis C, Karim M,

Rossignol D. Emerging biomarkers in autism spectrum disorder: a systematic review. Annals of translational medicine. 2019;7(23).

8. Tanner A, Dounavi K. The emergence of autism symptoms prior to 18 months of age: A systematic literature review. Journal of autism and developmental disorders. 2021;51(3):973-93.
9. Taberna GA, Samogin J, Mantini D. Automated head tissue modelling based on structural magnetic resonance images for electroencephalographic source reconstruction. Neuroinformatics. 2021;19(4):585-96.
10. Fischl B. FreeSurfer. NeuroImage. 2012;62(2):774-81.
11. Hashem S, Nisar S, Bhat AA, Yadav SK, Azeem MW, Bagga P, et al. Genetics of structural and functional brain changes in autism spectrum disorder. Translational Psychiatry. 2020;10(1):1-17.
12. Zhao X, Zhu S, Cao Y, Cheng P, Lin Y, Sun Z, et al. Abnormalities of Gray Matter Volume and Its Correlation with Clinical Symptoms in Adolescents with High-Functioning Autism Spectrum Disorder. Neuropsychiatr Dis Treat. 2022;18:717-30.
13. Riddle K, Cascio CJ, Woodward ND. Brain structure in autism: a voxel-based morphometry analysis of the Autism Brain Imaging Database Exchange (ABIDE). Brain imaging and behavior. 2017;11:541-51.
14. Lange N, Travers BG, Bigler ED, Prigge MB, Froehlich AL, Nielsen JA, et al. Longitudinal volumetric brain changes in autism spectrum disorder ages 6-35 years. Autism research : official journal of the International Society for Autism Research. 2015;8(1):82-93.
15. Courchesne E, Bartholomeusz H, Karns C, Townsend J. MRI and head circumference evidence of abnormal brain enlargement in young but not adult autistic patients. Biol Psychiatry.
16. Ni H-C, Lin H-Y, Tseng W-YI, Chiu Y-N, Wu Y-Y, Tsai W-C, et al. Neural correlates of impaired self-regulation in male youths with autism spectrum disorder: A voxel-based morphometry study. Progress in neuro-psychopharmacology and biological psychiatry. 2018;82:233-41.
17. Sato W, Kochiyama T, Uono S, Yoshimura S, Kubota Y, Sawada R, et al. Reduced gray matter volume in the social brain network in adults with autism spectrum disorder. Frontiers in human neuroscience. 2017;11:395.
18. Hanaie R, Mohri I, Kagitani-Shimono K, Tachibana M, Matsuzaki J, Hirata I, et al. White matter volume in the brainstem and inferior parietal lobule is related to motor performance in children with autism spectrum disorder: A voxel-based morphometry study. Autism Research. 2016;9(9):981-92.
19. Duerden EG, Mak-Fan KM, Taylor MJ, Roberts SW. Regional differences in grey and white matter in children and adults with autism spectrum disorders: An activation likelihood estimate (ALE) meta-analysis. Autism Research. 2012;5(1):49-66.
20. Zhao X, Zhu S, Cao Y, Cheng P, Lin Y, Sun Z, et al. Abnormalities of Gray Matter Volume and Its Correlation with Clinical Symptoms in Adolescents with High-Functioning Autism Spectrum Disorder. Neuropsychiatric Disease

and Treatment. 2022;18:717.

21. Haar S, Berman S, Behrmann M, Dinstein I. Anatomical abnormalities in autism? Cerebral cortex. 2016;26(4):1440-52.
22. Zielinski BA, Prigge MB, Nielsen JA, Froehlich AL, Abildskov TJ, Anderson JS, et al. Longitudinal changes in cortical thickness in autism and typical development. Brain. 2014;137(6):1799-812.
23. Nunes AS, Vakorin VA, Kozhemiako N, Peatfield N, Ribary U, Doesburg SM. Atypical age-related changes in cortical thickness in autism spectrum disorder. Scientific reports. 2020;10(1):1-15.
24. Jiao Y, Chen R, Ke X, Chu K, Lu Z, Herskovits EH. Predictive models of autism spectrum disorder based on brain regional cortical thickness. NeuroImage. 2010;50(2):589-99.
25. Khundrakpam BS, Lewis JD, Kostopoulos P, Carbonell F, Evans AC. Cortical thickness abnormalities in autism spectrum disorders through late childhood, adolescence, and adulthood: a large-scale MRI study. Cerebral Cortex. 2017;27(3):1721-31.
26. Bethlehem RA, Seidlitz J, Romero-Garcia R, Trakoshis S, Dumas G, Lombardo MV. A normative modelling approach reveals age-atypical cortical thickness in a subgroup of males with autism spectrum disorder. Communications biology. 2020;3(1):1-10.
27. Mei T, Llera A, Floris DL, Forde NJ, Tillmann J, Durston S, et al. Gray matter covariations and core symptoms of autism: the EU-AIMS Longitudinal European Autism Project. Molecular autism. 2020;11(1):1-13.
28. Maier S, van Elst LT, Perlov E, Düppers AL, Nickel K, Fangmeier T, et al. Cortical properties of adults with autism spectrum disorder and an IQ> 100. Psychiatry Research: Neuroimaging. 2018;279:8-13.
29. Mishra M, Pati UC. Autism detection using surface and volumetric morphometric feature of sMRI with Machine learning approach. 2021.
30. Seiger R, Ganger S, Kranz GS, Hahn A, Lanzenberger R. Cortical thickness estimations of FreeSurfer and the CAT12 toolbox in patients with Alzheimer's disease and healthy controls. Journal of Neuroimaging. 2018;28(5):515-23.
31. Maisel H, Eack S. Psychiatric Comorbidity and Neuromorphometry in Adults With Autism Spectrum Disorder. Biological Psychiatry. 2020;87(9):S326-S7.
32. Wolff N, Stroth S, Kamp-Becker I, Roepke S, Roessner V. Autism Spectrum Disorder and IQ–A Complex Interplay. Frontiers in Psychiatry. 2022;13:856084.
33. Chan W, Smith LE, Hong J, Greenberg JS, Mailick MR. Validating the social responsiveness scale for adults with autism. Autism Research. 2017;10(10):1663-71.
34. Ganji Z, Hakak MA, Zamanpour SA, Zare H. Automatic Detection of Focal Cortical Dysplasia Type II in MRI: Is the Application of Surface-Based Morphometry and Machine Learning Promising? Frontiers in Human Neuroscience. 2021;15.
35. Ganji Z, Aghaee Hakak M, Zare H. Comparison of machine learning methods for the detection of focal cortical dysplasia lesions: decision tree, support vector machine and artificial neural network. Neurological research. 2022;44(12):1142-9.

36. Ashburner J, Friston KJ. Unified segmentation. NeuroImage. 2005;26(3):839-51.
37. Klein A, Andersson J, Ardekani BA, Ashburner J, Avants B, Chiang MC, et al. Evaluation of 14 nonlinear deformation algorithms applied to human brain MRI registration. NeuroImage. 2009;46(3):786-802.
38. Ay U, Kizilates-Evin G, Bayram A, Kurt E, Demiralp T. Comparison of FreeSurfer and CAT12 Software in Parcel-Based Cortical Thickness Calculations. Brain topography. 2022;35(5-6):572-82.
39. Yotter RA, Dahnke R, Thompson PM, Gaser C. Topological correction of brain surface meshes using spherical harmonics. Hum Brain Mapp. 2011;32(7):1109-24.
40. Khadem-Reza ZK, Zare H. Evaluation of brain structure abnormalities in children with autism spectrum disorder (ASD) using structural magnetic resonance imaging. The Egyptian Journal of Neurology, Psychiatry and Neurosurgery. 2022;58(1):1-14.
41. Desikan RS, Ségonne F, Fischl B, Quinn BT, Dickerson BC, Blacker D, et al. An automated labeling system for subdividing the human cerebral cortex on MRI scans into gyral based regions of interest. NeuroImage. 2006;31(3):968-80.
42. Hammers A, Allom R, Koepp MJ, Free SL, Myers R, Lemieux L, et al. Three-dimensional maximum probability atlas of the human brain, with particular reference to the temporal lobe. Human brain mapping. 2003;19(4):224-47.
43. Desikan RS, Ségonne F, Fischl B, Quinn BT, Dickerson BC, Blacker D, et al. An automated labeling system for subdividing the human cerebral cortex on MRI scans into gyral based regions of interest. NeuroImage. 2006;31(3):968-80.
44. Greimel E, Nehrkorn B, Schulte-Rüther M, Fink GR, Nickl-Jockschat T, Herpertz-Dahlmann B, et al. Changes in grey matter development in autism spectrum disorder. Brain Structure and Function. 2013;218(4):929-42.
45. Uddin LQ, Supekar K, Menon V. Reconceptualizing functional brain connectivity in autism from a developmental perspective. Frontiers in human neuroscience. 2013;7:458.
46. O'Hearn K, Larsen B, Fedor J, Luna B, Lynn A. Representational similarity analysis reveals atypical age-related changes in brain regions supporting face and car recognition in autism. NeuroImage. 2020;209:116322.
47. Murphy CM, Deeley Q, Daly E, Ecker C, O'brien F, Hallahan B, et al. Anatomy and aging of the amygdala and hippocampus in autism spectrum disorder: an in vivo magnetic resonance imaging study of Asperger syndrome. Autism Research. 2012;5(1):3-12.
48. Yang DY-J, Beam D, Pelphrey KA, Abdullahi S, Jou RJ. Cortical morphological markers in children with autism: a structural magnetic resonance imaging study of thickness, area, volume, and gyrification. Molecular autism. 2016;7(1):1-14.
49. Riddle K, Cascio CJ, Woodward ND. Brain structure in autism: a voxel-based morphometry analysis of the Autism Brain Imaging Database Exchange (ABIDE). Brain imaging and behavior. 2017;11(2):541-51.
50. Kucharsky Hiess R, Alter R, Sojoudi S, Ardekani B, Kuzniecky R, Pardoe H. Corpus

callosum area and brain volume in autism spectrum disorder: quantitative analysis of structural MRI from the ABIDE database. Journal of autism and developmental disorders. 2015;45(10):3107-14.

51. Katuwal GJ, Baum SA, Michael AM. Early brain imaging can predict autism: Application of machine learning to a clinical imaging archive. BioRxiv. 2018:471169.
52. Xiao Z, Qiu T, Ke X, Xiao X, Xiao T, Liang F, et al. Autism spectrum disorder as early neurodevelopmental disorder: Evidence from the brain imaging abnormalities in 2–3 years old toddlers. Journal of autism and developmental disorders. 2014;44(7):1633-40.
53. Katuwal GJ, Baum SA, Cahill ND, Dougherty CC, Evans E, Evans DW, et al. Inter-method discrepancies in brain volume estimation may drive inconsistent findings in autism. Frontiers in neuroscience. 2016;10:439.
54. D'Mello AM, Crocetti D, Mostofsky SH, Stoodley CJ. Cerebellar gray matter and lobular volumes correlate with core autism symptoms. NeuroImage Clinical. 2015;7:631-9.
55. Hoffmann E, Brück C, Kreifelts B, Ethofer T, Wildgruber D. Reduced functional connectivity to the frontal cortex during processing of social cues in autism spectrum disorder. Journal of Neural Transmission. 2016;123(8):937-47.
56. Xu J, Wang C, Xu Z, Li T, Chen F, Chen K, et al. Specific functional connectivity patterns of middle temporal gyrus subregions in children and adults with autism spectrum disorder. Autism Research. 2020;13(3):410-22.
57. Sato W, Uono S. The atypical social brain network in autism: advances in structural and functional MRI studies. Current Opinion in Neurology. 2019;32(4):617-21.
58. Cauda F, Geda E, Sacco K, D'Agata F, Duca S, Geminiani G, et al. Grey matter abnormality in autism spectrum disorder: an activation likelihood estimation meta-analysis study. Journal of Neurology, Neurosurgery & Psychiatry. 2011;82(12):1304-13.
59. Yang X, Si T, Gong Q, Qiu L, Jia Z, Zhou M, et al. Brain gray matter alterations and associated demographic profiles in adults with autism spectrum disorder: A meta-analysis of voxel-based morphometry studies. Australian & New Zealand Journal of Psychiatry. 2016;50(8):741-53.
60. Wallace GL, Dankner N, Kenworthy L, Giedd JN, Martin A. Age-related temporal and parietal cortical thinning in autism spectrum disorders. Brain. 2010;133(12):3745-54.
61. Foster NE, Doyle-Thomas KA, Tryfon A, Ouimet T, Anagnostou E, Evans AC, et al. Structural gray matter differences during childhood development in autism spectrum disorder: a multimetric approach. Pediatric neurology. 2015;53(4):350-9.
62. Wallace GL, Eisenberg IW, Robustelli B, Dankner N, Kenworthy L, Giedd JN, et al. Longitudinal cortical development during adolescence and young adulthood in autism spectrum disorder: increased cortical thinning but comparable surface area changes. Journal of the American Academy of Child & Adolescent Psychiatry. 2015;54(6):464-9.
63. Iacoboni M. Neurobiology of imitation. Current opinion in neurobiology. 2009;19(6):661-5.
64. Miller E. Functional Connectivity of the

Inferior Frontal Gyrus in Autism Spectrum Disorders. 2021.

65. Cermak CA, Arshinoff S, Ribeiro de Oliveira L, Tendera A, Beal DS, Brian J, et al. Brain and Language Associations in Autism Spectrum Disorder: A Scoping Review. Journal of Autism and Developmental Disorders. 2021:1-13.
66. Yamasaki S, Yamasue H, Abe O, Suga M, Yamada H, Inoue H, et al. Reduced gray matter volume of pars opercularis is associated with impaired social communication in high-functioning autism spectrum disorders. Biol Psychiatry. 2010;68(12):1141-7.
67. McAlonan GM, Cheung V, Cheung C, Suckling J, Lam GY, Tai K, et al. Mapping the brain in autism. A voxel-based MRI study of volumetric differences and intercorrelations in autism. Brain. 2005;128(2):268-76.
68. Apps MA, Rushworth MF, Chang SW. The anterior cingulate gyrus and social cognition: tracking the motivation of others. Neuron. 2016;90(4):692-707.
69. Bzdok D, Hartwigsen G, Reid A, Laird AR, Fox PT, Eickhoff SB. Left inferior parietal lobe engagement in social cognition and language. Neuroscience & Biobehavioral Reviews. 2016;68:319-34.
70. Focquaert F, Vanneste S. Autism spectrum traits in normal individuals: a preliminary VBM analysis. Frontiers in Human Neuroscience. 2015;9:264.
71. Jung M, Tu Y, Lang CA, Ortiz A, Park J, Jorgenson K, et al. Decreased structural connectivity and resting-state brain activity in the lateral occipital cortex is associated with social communication deficits in boys with autism spectrum disorder. NeuroImage. 2019;190:205-12.
72. Oades RD. Frontal, temporal and lateralized brain function in children with attention-deficit hyperactivity disorder: a psychophysiological and neuropsychological viewpoint on development. Behavioural brain research. 1998;94(1):83-95.
73. Sato W, Toichi M, Uono S, Kochiyama T. Impaired social brain network for processing dynamic facial expressions in autism spectrum disorders. BMC neuroscience. 2012;13(1):1-17.
74. Scheel C, Rotarska-Jagiela A, Schilbach L, Lehnhardt FG, Krug B, Vogeley K, et al. Imaging derived cortical thickness reduction in high-functioning autism: key regions and temporal slope. NeuroImage. 2011;58(2):391-400.
75. Ecker C, Ginestet C, Feng Y, Johnston P, Lombardo MV, Lai M-C, et al. Brain surface anatomy in adults with autism: the relationship between surface area, cortical thickness, and autistic symptoms. JAMA psychiatry. 2013;70(1):59-70.
76. Hardan AY, Libove RA, Keshavan MS, Melhem NM, Minshew NJ. A preliminary longitudinal magnetic resonance imaging study of brain volume and cortical thickness in autism. Biological psychiatry. 2009;66(4):320-6.
77. Constantino J, Todorov A, Hilton C, Law P, Zhang Y, Molloy E, et al. Autism recurrence in half siblings: strong support for genetic mechanisms of transmission in ASD. Molecular psychiatry. 2013;18(2):137-8.
78. Smith E, Thurm A, Greenstein D, Farmer C, Swedo S, Giedd J, et al. Cortical thickness

change in autism during early childhood. Human brain mapping. 2016;37(7):2616-29.

79. Parikshak NN, Luo R, Zhang A, Won H, Lowe JK, Chandran V, et al. Integrative functional genomic analyses implicate specific molecular pathways and circuits in autism. Cell. 2013;155(5):1008-21.
80. Luo W, Zhang C, Jiang Y-h, Brouwer CR. Systematic reconstruction of autism biology from massive genetic mutation profiles. Science advances. 2018;4(4):e1701799.
81. Sanders SJ, Murtha MT, Gupta AR, Murdoch JD, Raubeson MJ, Willsey AJ, et al. De novo mutations revealed by whole-exome sequencing are strongly associated with autism. Nature. 2012;485(7397):237-41.
82. Sala C, Vicidomini C, Bigi I, Mossa A, Verpelli C. Shank synaptic scaffold proteins: keys to understanding the pathogenesis of autism and other synaptic disorders. Journal of neurochemistry. 2015;135(5):849-58.
83. Li D, Karnath H-O, Xu X. Candidate biomarkers in children with autism spectrum disorder: a review of MRI studies. Neuroscience bulletin. 2017;33:219-37.
84. Kharabian Masouleh S, Eickhoff SB, Zeighami Y, Lewis LB, Dahnke R, Gaser C, et al. Influence of processing pipeline on cortical thickness measurement. Cerebral Cortex. 2020;30(9):5014-27.
85. Pulli EP, Silver E, Kumpulainen V, Copeland A, Merisaari H, Saunavaara J, et al. Feasibility of FreeSurfer processing for T1-weighted brain images of 5-year-olds: semiautomated protocol of FinnBrain Neuroimaging Lab. Frontiers in Neuroscience. 2022;16:874062.